This article has been accepted for publication in IEEE Control Systems Letters. This is the author's version which has not been fully edited and content may change prior to final publication. Citation information: DOI 10.1109/LCSYS.2023.3336545

Iterative Learning Embedded Composite Model Reference Adaptive Control for Off-axis In-situ Rotation in Nanorobotic Manipulation

Heng Zhang, Xiang Fu, Song Liu, *Member, IEEE,* Yang Wang, *Member, IEEE*

***Abstract*— Realizing dexterous rotation under the microscope has been a great and yet not-well-addressed challenge in micro/nano-robotics. The limited field of view (FOV) of a microscope necessitates point-wise in-situ rotation, which refers to manipulating objects within their existing or natural environment. Though *on-axis* in-situ rotation has been investigated, *off-axis* in-situ rotation, which is more suitable to classical nano-robot setups, remains unexplored. The main difficulty facing here is the model uncertainties and visual disturbances that fail traditional control methods. In this paper, we propose a novel control scheme, namely the iterative learning embedded composite model reference adaptive control (IL-CMRAC), for efficient visual servo to solve the problem of in-situ off-axis rotation, by fully leveraging the repetitiveness nature of rotational motion. IL-CMRAC takes advantage of both offline learning and online adaptation to tackle the difficulties brought by uncertainties. Experiments demonstrated that the proposed method is capable of realizing high-precision off-axis in-situ rotation by average error within several microns.**

***Index Terms*— Nanorobotics, Indirect Iterative Learning Control, Composite Model Reference Adaptive Control**

I. Introduction

NANOROBOTIC manipulation under the microscope has greatly extended mankind's capability in handling micro/nano-scale objects in material [1] and life science [2], particularly in terms of in-situ characterization and in-situ manipulation [3]. Among different in-situ tasks, in-situ rotation has been a great challenge in nanorobotics, which can find wide applications like 360° materials observation or twisting test [4]. By mechanical setup, in-situ rotation can be realized by on-axis rotating [5] or off-axis rotating, depending on whether the target point sits on the rotating axis. With on-axis in-situ rotation has been well investigated, however, off-axis in-situ rotation is more intuitive and versatile but remains unexplored. The staggering challenge is that the eye-hand model uncertainties and nonlinear mechanical disturbances become prominent leading to large spatial misalignment errors. Thus, the necessity to develop a suitable control method for *off-axis* in-situ rotation arises for the nanorobotics community.

*This work was in part supported by the NSFC under Grant 62303321 and the Yangfan Program under Grant 21YF1429600. (Heng Zhang and Xiang Fu contribute equally to this work.) (Corresponding authors: Song Liu and Yang Wang.)

H. Zhang, X. Fu, S. Liu, and Y. Wang are with the School of Information Science and Technology, ShanghaiTech University, Shanghai, China {zhangheng1, fuxiang2022, liusong, wangyang4@shanghaitech.edu.cn}

Numerous methods have been developed in the control community to address the challenge stemming from the model uncertainties and external disturbances. However, these methods have not leveraged the inherent repetitiveness of many robotics systems, leading to unsatisfactory transient performance for motion control [6]. Such an issue can be effectively addressed by the Iterative Learning Control (ILC). Nonetheless, conventional ILC is unable to address scenarios that feature complicated uncertainties [7], such as non-identical initial conditions, or batch-varying dynamics. Traditional ILC [8] can only guarantee bounded iterative convergence, if those uncertainties between iterations are bounded. Alternatively, adaptive control exhibits a notable efficacy in dealing with non-repetitive uncertainties. Among various existing solutions, the composite model reference adaptive control (CMRAC) strategy [9] stands out as one of the most renowned and mature methodologies. Compared to the conventional MARC, CMARC uses both prediction errors and tracking errors in formulating adaptive law dynamics and therefore exhibits better transient characteristics and improves parameter convergence [9]–[11]. The inherent constraint confines the CMRAC approach to tracking the output of the reference model rather than directly tracking the reference signal itself. However, similar to any model reference adaptive technique, crafting a reference model capable of eliciting intended responses across diverse trajectories remains a formidable challenge even for seasoned control engineers. Regardless of some attempts [12]–[15] to combine the ILC and adaptive control, there is few approach that fully exploits the online data memory to extract parametric information such that the convergence of the tracking error and prediction error can be simultaneously guaranteed without a stringent condition termed persistent excitation.

Motivated by the above discussion, we propose a novel IL-CMRAC framework that combines the ILC and CMRAC techniques to solve the off-axis in-situ rotation problem of nanorobots *in precision scale*. The delicate integration of learning and adaptive control relies on the introduction of a stabilized nominal model as the reference model. This allows us to obtain the learning policy in an offline and low-cost manner and endows the controller with the direct ability to track the desired reference signal. Furthermore, the proposed scheme, not only relaxes the stringent repetitive conditions imposed by ILC assumptions but also reduces the effort of designing reference models, thus mitigating the need for extensive control expertise.

This article has been accepted for publication in IEEE Control Systems Letters. This is the author's version which has not been fully edited and content may change prior to final publication. Citation information: DOI 10.1109/LCSYS.2023.3336545

Notation: Defined $\mathbb{Z} = \{0, 1, 2, 3, \cdots\}$ as the set of integer, and similarly, $\mathbb{Z}_+ = \{1, 2, \cdots\}$, $\mathbb{Z}_N = \{0, 1, \cdots, N\}$, $\mathcal{I}_m = \{1, 2, \cdots, m\}$ for some $N, m \in \mathbb{Z}_+$. The symbol z is used to denote the advance operator: $z[\![r(t)]\!] = r(t+1)$, and $W_m(z)[\![r(t)]\!]$ denotes the time-domain output of the system $W_m(z)$ whose input is $r(t)$. $I_m \in \mathbb{R}^{m\times m}$ is used to denote the identical matrix.

II. Nanorobots and Problem Formulation

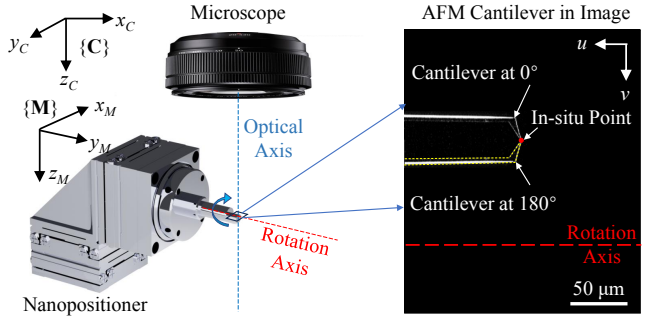

Fig. 1. Illustration of off-axis in-situ rotation of nanorobot under the microscope. Note the in-situ point is away from the rotating axis. The coordinates **{M}** is established on nanopositioner, while coordinates **{C}** is established on microscope.

In order to maintain in-situ of the observed object during rotation under scanning electron microscope, a nanorobotic system is established, consisting of a microscope providing visual feedback and a nanopositioner composed of three translation degrees of freedom (DOFs) and a rotation DOF, as illustrated by Fig. 1. The three translation DOFs are orthogonally mounted, with the rotation DOF utilized at the end joint of the nanopositioner. The nanopositioners are driven based on the stick-slip effect of piezoelectric ceramic material and provide precise optical grating feedback with repeatability accuracy of 50 nm and 1 m°. The rotary nanopositioner rotates the observed sample around one axis, changing its posture and giving multidirectional imaging condition under microscope, and the translational nanopositioners provide linear movement along the three axes, compensating on the displacement during rotation. In this experiment, an atomic force microscope (AFM) cantilever is securely fixed on the end of the nanopositioner with an unknown mechanical misalignment away from the rotation axis. The off-axis in-situ rotation task is thus specifically described as: The nanopositioner keeps rotating while the AFM cantilever tip is fixed in a specific spatial location (in-situ point) by compensating the misalignment errors from the image through the translation DOFs.

In virtue of [16], the nanorobot system is modelled by:

$$\begin{aligned} x(t+1) &= Ax(t) + B[u(t) + f(t) + E\sum_{i=0}^{t-1} u(i)] \\ y(t) &= Cx(t) \end{aligned} \tag{1}$$

where $x(t) \in \mathbb{R}^3$, and $u(t) \in \mathbb{R}^3$ are state and input of system, respectively. $y(t) \in \mathbb{R}^2$ are output signals which is measured by SEM. $A \in \mathbb{R}^{3\times3}, C \in \mathbb{R}^{2\times3}, E \in \mathbb{R}^{3\times3}$ are model matrices and $B \in \mathbb{R}^{3\times3}$ is an identity matrix. $f(t)$ is a nonlinear term representing external disturbances and unmodeled factors.

Remark 1: With the ideal mechanical setup of the nanorobot, the cantilever exhibits identical motion trajectories with continuous rotation. Consequently, the in-situ control challenge of the nanorobot is characterized by iterative repetitions. In (1), the variable t represents the angular increment of the rotation joint during each rotation, commonly taking values of 1 degree, 2 degrees, or 5 degrees.

The control objective is now described as: the output $y(t)$ in system (1) is desired to remain constant, consistent with its initial value. To address such problems, we rewrite system (1) in more general multi-input and multi-output (MIMO) nonlinear form:

$$\begin{aligned} x(k,t+1) =& A(k)x(k,t) + B(k)(u(k,t) + \theta^\top(k)\phi(x(k,t),t)), \\ y(k,t+1) =& C_0 x(k,t+1), \quad x(k,0) = x_k \end{aligned} \tag{2}$$

where $t \in \mathbb{Z}_N$ and $k \in \mathbb{Z}_+$, respectively, denote the time and iteration index. $x_k \in \mathbb{R}^n$ represent the unknown initial states at k-th batch.

The system is considered to be an iterative-varying one in the sense that $A(k) = A_0 + \Delta A(k)$ and $B(k) = B_0 + \Delta B(k)$, in which A_0 and B_0 are the nominal part of $A(k)$ and $B(k)$, $\Delta A(k)$ and $\Delta B(k)$ are the corresponding uncertainties in the k-th iteration. A_0, B_0, C_0 are assumed iteration-invariant and known. In this letter, the effects caused by nonlinear term $f(t)$ and cumulative input $E\sum_{i=0}^{t-1} u(k,i)$ are expressed as a static parametric model (SPM), i.e. $\theta^\top(k)\phi(x,t)$. $\theta(k) \in \mathbb{R}^{s\times m}$ is an unknown constant matrix and $\phi(x,t) \in \mathbb{R}^{s\times1}$ is a bounded and known vector depending on the state. For future use, define $G_k(z) := C_0(zI - A(k))^{-1}B(k)$, and Δ_i is utilized to represent the leading principal minors of the high-frequency gain matrix of $G_k(z)$, for all $i \in \mathcal{I}_m$. To proceed, some assumptions are made as follows:

Assumption 1: $(A(k), B(k), C_0)$ and (A_0, B_0, C_0) are stabilizable and detectable for all $k \in \mathbb{Z}_+$. Furthermore, the matrix B_0 is a full rank matrix. ◁

Assumption 2: [17] $G_k(z)$ is a full-rank matrix with all its zeros located in the unit circle in the z-plane for all $k \in \mathbb{Z}_+$. For all $i \in \mathcal{I}_m$, Δ_i are nonzero, and $\mathrm{sgn}(\Delta_i)$ is known. ◁

Remark 2: Assumption 1 is crucial for ensuring the solvability of the rotation task and for preserving internal stability within the system. Assumption 2 essentially captures characteristics of the zero structure of the system transfer matrix $G_k(z)$ at infinity ($z = \infty$) and therefore is required for stable zero-pole cancellations in plant-model matching (see (8)), and is used for constructing a common reference model transfer matrix $W_m(z)$. The assumptions made regarding the nanorobot signify its' capability to execute precise and stable manipulation, facilitating the feedback control design.

Now, the off-axis in-situ control problem is cast as:

Problem 1: Suppose Assumptions 1-2 hold. For repetitive system (2) with bounded model uncertainties and external disturbances, design a control scheme such that for any initial state of the system, all the signals of the closed-loop system are bounded and the system output signals $y(k,t)$ asymptotically track a desired trajectories[1] $y_d(t)$ as $k \to \infty$. ◁

[1]For off-axis in-situ rotation of the nanorobotic manipulation considered, the desired trajectory is its initial position $y_d(t) = y_d(0)$ for all $t \in \mathbb{Z}_N$

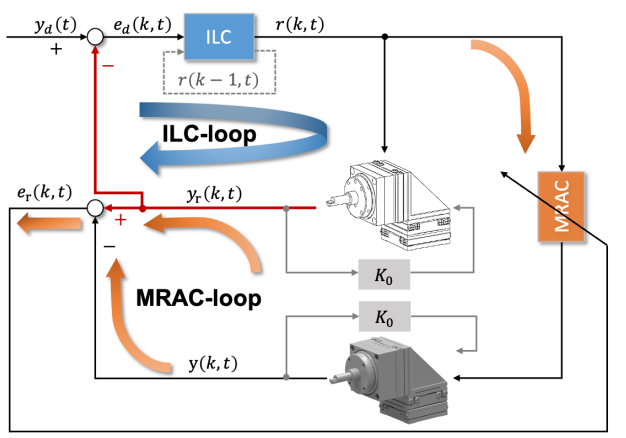

Fig. 2. Schematic of the proposed IL-CMARC scheme.

III. Controller Design and Stability Analysis

A. Controller Design

First, in virtue of (2), the reference model is given by

$$\begin{aligned} x_r(k,t+1) &= A_r x_r(k,t) + B_0 r(k,t), \\ y_r(k,t+1) &= C_0 x_r(k,t+1), \quad x_r(k,0) = x_0 \in \mathbb{R}^n \end{aligned} \tag{4}$$

where $r(k,t) \in \mathbb{R}^m$ is a reference signal provided by an IL update law in (5), $x_0 \in \mathbb{R}^n$ represent the initial states demanded by users. $A_r = A_0 + B_0 K_0$ is a Schur matrix that is stabilized by a proper gain matrix $K_0 \in \mathbb{R}^{m\times n}$. Since the controllability of (A_0, B_0) is hypothesized in Assumption 1, the existence of K_0 is ensured. Note that, if we recast system (4) as $y_r(k,t) = W_m(z)[\![r(k,t)]\!]$ with $W_m(z) = C_0(zI - A_r)^{-1}B_0$, there exists a finite and non-singular matrix K_p [17] such that $K_p = \lim_{z\to\infty} W_m^{-1}(z)G_k(z)$ for all $k \in \mathbb{Z}_+$.

System (4) plays the role of a 'reference' in the sense that we wish the state of Plant (2) to asymptotically track the state of (4) via the adaptive control law. However, in contrast to conventional MARC, here, the design of K_0 is rather simple as we only need to render the A_r matrix to be Shur. It implies that the proposed scheme does not require a delicate design of K_0 to balance the performance specifications such as the transient behavior, settling time, steady-state error, etc. Instead, we tend to achieve an 'optimal' behavior via an iterative learning procedure. That is, we will find $r(k,t)$ such that $y_r(k,t) \to y_d(t)$ as $k \to \infty$. To achieve this, it is natural to assume the desired trajectory $y_d(t)$ is realizable.

Assumption 3: There exists a bounded state sequence $x_d(t)$ and a unique bounded input sequence $r_d(t)$ that satisfy

$$\begin{aligned} x_d(t+1) &= A_r x_d(t) + B_0 r_d(t) \\ y_d(t+1) &= C_0 x_d(t), \end{aligned}$$

with $x_d(k,0) = x_0 \in \mathbb{R}^n$. ◁

Now, the IL update law at k-th operation cycle is given by

$$r(k+1,t) = r(k,t) + K_r(t)[x_d(t) - x_r(k,t)], \tag{5}$$

where $K_r(t) \in \mathbb{R}^{m\times m}$ is a learning gain matrix that verifies the following condition [18]

$$\|I - K_r(t)B_0\| \le \rho < 1\ , \quad \forall t \in \mathbb{Z}_N \tag{6}$$

where $\rho \in [0,1)$ is a constant. Note that, since the reference model is purely numerical, one can easily obtain an IL update law $r(k,t)$ achieving a high precision tracking.

As shown in Fig. 2, with the IL-loop enabling $y_r(k,t)$ to track $y_d(t)$, the original problem has now been shifted to steer the output of system (2) to track the output of system (4), i.e. $y(k,t) \to y_r(k,t)$ as $t \to \infty$. The main challenge of transferring the learned policy from the reference model to a physical one arises from the model uncertainties, external disturbances and iteration-varying initial states, which are tackled by the following CMARC law:

$$u(k,t) = K_1(k,t)x(k,t) + K_2(k,t)r(k,t) - \hat{\theta}^\top(k,t)\phi(x) \tag{7}$$

where $\hat{\theta}(k,t)$ is the adaptive estimate of the unknown compensation term θ. $K_1(k,t) := K_0 + K_x(k,t)$ with some matrix $K_x(k,t) \in \mathbb{R}^{m\times n}$, and $K_2(k,t) \in \mathbb{R}^{m\times m}$ are the estimates of $K_1^*(k)$ and $K_2^*(k)$, which satisfy the matching condition [19]:

$$C_0(zI - A - BK_1^{*\top})^{-1}BK_2^* = W_m(z)\ ,\ K_2^{*-1} = K_p \tag{8}$$

Further, the accessibility of the state $x(k,t)$ is assumed or provided by an observer, such as a Kalman observer [20] and extended state observer [21]. The convergence of the observation error is not discussed here, due to space limitations.

Next, we are going to develop the update laws for the matrices $K_2(k,t)$, $K_x(k,t)$, and $\hat{\theta}^\top(k,t)$. For the simplicity of the notation, let us first define

$$\begin{aligned} \Theta^\top(k,t) &:= \left[K_1(k,t), K_2(k,t), \hat{\theta}^\top(k,t)\right] \in \mathbb{R}^{m\times(n+m+s)} \\ \Theta^{*\top}(k) &:= \left[K_1^*, K_2^*, \theta^\top\right], \quad \tilde{\Theta}(k,t) := \Theta(k,t) - \Theta^*(k). \end{aligned}$$

Substituting the controller (7) in the plant (2), together with (4) and (8), we have the output tracking error equation

$$e_r(k,t) = y(k,t) - y_r(k,t) = W_m(z)K_p[\![\tilde{\Theta}^\top\omega(k,t)]\!] \tag{9}$$

with $\omega(k,t) = \left[x^\top(k,t), r^\top(k,t), -\phi^\top(x,t)\right]^\top$.

Now, we present the composite updated law as follows

$$\Theta^\top(k,t+1) = \Theta^\top(k,t) - \frac{D\epsilon(k,t)\zeta^\top(k,t)}{m^2(k,t)}, \tag{10}$$

$$\beta_i(k,t+1) = \beta_i(k,t) - \frac{\Gamma_{\beta i}\epsilon_i(k,t)\eta_i(k,t)}{m^2(k,t)}, \tag{11}$$

$$\Psi(k,t+1) = \Psi(k,t) - \frac{\Gamma\epsilon(k,t)\xi^\top(k,t)}{m^2(k,t)}, \tag{12}$$

$$\begin{aligned} \epsilon(k,t) &= \left[0, \beta_2^\top\eta_2, \ldots, \beta_m^\top\eta_m\right]^\top(k,t) + \Psi(k,t)\xi(k,t) + \bar{e}_r(k,t) \\ &= \underbrace{\left[\eta_2, \tilde{\beta}_2'^\top\eta_3, \ldots, \tilde{\beta}_m'^\top\eta_{m+1}\right]^\top(k,t) + \tilde{\Psi}(k,t)\xi(k,t) + DS(k)\tilde{\Theta}^\top(k,t)\zeta(k,t)}_{\text{prediction error}} - \underbrace{\bar{e}_r(k,t)}_{\text{tracking error}} \end{aligned} \tag{3}$$

where $0 < \Gamma_{\beta i} = \Gamma_{\beta i}^{\top} < 2I_{i-1}, i = 2, \ldots, m, 0 < \Gamma = \Gamma^{\top} < 2I_m$, D is chosen to satisfy $0 < DSD < 2I_m$, S is a symmetric positive definite matrix defined later, and $m(k,t) = \sqrt{1 + \zeta^{\top}\zeta(k,t) + \xi^{\top}\xi(k,t) + \sum_{i=2}^{m} \eta_i^{\top}\eta_i(k,t)}$. The composite error signals $\epsilon = [\epsilon_1, \ldots, \epsilon_m]^{\top}$ and filtered tracking error $\bar{e}_r = [\bar{e}_{r,1}, \ldots, \bar{e}_{r,m}]^{\top}$ are computed in (3) (refer to the detailed derivation process in Supplementary Material (SM) Section III) and

$$\begin{aligned} \bar{e}_r(k,t) &= W_m^{-1}(z)h(z)[\![e_r(k,t)]\!], \\ \xi(k,t) &= \Theta^{\top}(k,t)\zeta(k,t) - h(z)[\![\Theta^{\top}\omega(k,t)]\!], \\ \zeta(k,t) &= h(z)[\![\omega(k,t)]\!] \\ \eta_i(k,t) &= [\bar{e}_{r,1}, \ldots, \bar{e}_{r,i-1}]^{\top}(k,t), \end{aligned} \tag{13}$$

with $h(z) = 1/f_h(z)$, where $f_h(z)$ is a stable and monic polynomial of degree that equals the degree of $W_m^{-1}(z)$. $\beta_i(k,t) \in \mathbb{R}^{(i-1)\times 1}$ and $\Psi(k,t) \in \mathbb{R}^{m\times m}$ are respectively the estimate of $\beta_i^*(k) = [\beta_{i,1}^*, \ldots, \beta_{i,i-1}^*]^{\top}(k)$, $i = 2, \ldots, m$, and $\Psi^*(k) = DS(k)$ in the k-th iteration. $\beta_{i,j}^*(k) = L^{-1}(k) - I_m$ with $\beta_{i,j}^*(k) = 0$ for $i \in \mathcal{I}_m$ and $j \geq i$. $L(k)$, D and $S(k)$ are the LDS decomposition [22] of $K_p(k)$, i.e. $K_p(k) = L(k)DS(k)$. It is worth noting that, from Assumption 2, there exists a matrix D for the piecewise constant matrix $K_p(k)$ for all $k \in \mathbb{Z}_+$. The estimation error are defined as $\tilde{\beta}_i'(k,t) = [\tilde{\beta}_i^{\top}, 1]^{\top}(k,t) = [(\beta_i - \beta_i^*)^{\top}, 1]^{\top}(k,t)$ for $i = 2, \ldots, m$, and $\tilde{\Psi}(k,t) = \Psi(k,t) - \Psi^*(k)$.

Remark 3: The uniqueness of our composite adaptive law lies in its fusion of predictive modeling and tracking error feedback. This innovative approach allows us to leverage hidden parametric information within prediction errors, enhancing both trajectory tracking and parameter estimation.

Remark 4: At k-th iteration, the adaptive laws (10)-(12) ensure that 1) $\beta_i(t) \in l_\infty, i = 2, 3, \ldots, m, \Theta(t) \in l_\infty, \Psi(t) \in l_\infty$, and $\frac{\epsilon(t)}{m(t)} \in l_2 \cap l_\infty$, which implies that $\lim_{t\to\infty} \epsilon(t) = 0$; 2) $\beta_i(t+1) - \beta_i(t) \in l_2 \cap l_\infty, i = 2, 3, \ldots, m, \Theta(t+1) - \Theta(t) \in l_2 \cap l_\infty$, and $\Psi(t+1) - \Psi(t) \in l_2 \cap l_\infty$. The proof of these statements is given in SM Section V.

Let $\tilde{\Theta}_r = \text{diag}(\tilde{\Theta}^{\top}, [\tilde{\beta}_2, \cdots, \tilde{\beta}_m]^{\top}, \tilde{\Phi})$. In view of (10)-(12), one can obtain

$$\tilde{\Theta}_r(k, t+1) = \tilde{\Theta}_r(k,t) - \Gamma_r \epsilon_r \Phi_r / m^2(k,t)$$

with $\Gamma_r = \text{diag}(D, \Gamma_{\beta 2}, \cdots, \Gamma_{\beta m}, \Gamma)$, $\epsilon_r = \text{diag}(\epsilon, \epsilon_2 I_1, \cdots, \epsilon_m I_{m-1}, \epsilon)$ and $\Phi_r = \text{diag}(\zeta^{\top}, [\eta_2, \cdots, \eta_m]^{\top}, \xi^{\top})$. Consider the case when $\frac{\Gamma_r \epsilon_r \Phi_r}{m^2}(k,t)$ satisfies the PE condition, defined in Definition 1 in SM Section I, the estimation error $\tilde{\Theta}_r$ will exponentially converge to zero.

B. Brief Stability Analysis

Define $e_d(k,t) = y_d(t) - y_r(k,t)$ and $e(k,t) = y_d(t) - y(k,t)$. According to the above analysis, we are now in a position to state the main results of this article.

Theorem 3.1: Suppose Assumptions 1-3 hold for system (2). For any $\epsilon_d > 0$, $t \in \mathbb{Z}_N$ and $k \geq k^*$ with some $k^* \in \mathbb{Z}_+$, the proposed IL-CMARC scheme guarantees that all signals of the closed-loop system described by (2), (5), (7), (10)-(12) are bounded and $\lim_{t\to\infty} \|e(k,t)\| \leq \epsilon_d$, if the condition (6) is satisfied.

Proof: In view of (9), it is easy to see that $e(k,t) = e_d(k,t) - e_r(k,t)$. On the one hand, given condition (6), the proof of the zero convergence of $e_d(k,t)$ follows a standard procedure of compression mapping that is similar to the proof of Theorem 3 in [23] and hence is omitted here due to space limitation (see SM Section II for more detail). Therefore, for any $\epsilon_d > 0$, $t \in \mathbb{Z}_N$, there exists a constant $k^* \in \mathbb{Z}_+$ such that for all $k \geq k^*$, $\|e_d(k,t)\| < \epsilon_d$. On the other hand, according to error equation (9), the convergence of tracking error $e_r(k,t)$ is guaranteed by analyzing signal transmission and using the small gain theorem (see Lemma 3 in SM Section I for detail). In the process, the boundedness of all signals is also ensured.

Finally, we can conclude that

$$\|e(k,t)\| \leq \|e_d(k,t)\| + \|e_r(k,t)\| < \epsilon_d + \|e_r(k,t)\| \tag{14}$$

for all $k \geq k^*$. Taking the limit of $t \to \infty$ on both side of (14), we have $\lim_{t\to\infty} \|e(k,t)\| \leq \epsilon_d$. ■

Remark 5: Note that, we choose to present our convergence property in the time domain, rather than the iteration domain, which is primarily motivated by the consideration of our nanorobot system's mechanical configuration. Although off-axis in-situ rotation follows a recurring and iterative pattern, the control objective primarily focuses on time-domain convergence, given the continuous nature of the motion trajectory and the inherent time-varying nature of uncertainties.

IV. Experiment Results

A. Nanorobot Setup

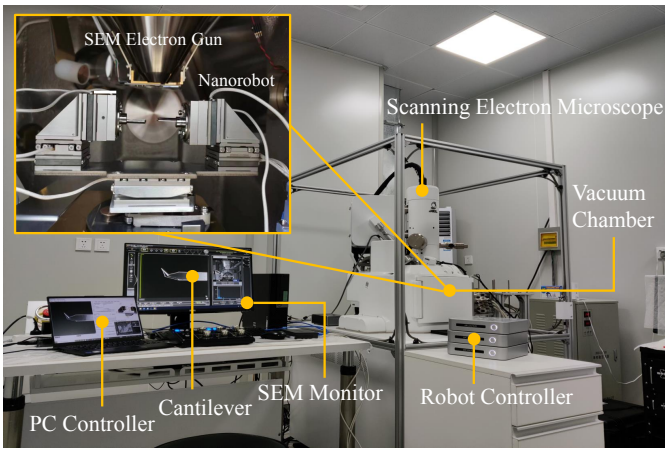

Fig. 3. The testing nanorobot system. Overall view and close view(top-left subfigure) of nanopositioner mounted in the SEM vacuum chamber.

Fig. 3 shows the testing nanorobot under a scanning electron microscope (SEM). The SEM was JEOL JSM-IT500HR/LA, working at high vacuum mode for imaging through detecting secondary electrons, under 10 KV acceleration voltage, which captures 7 frames per second with an image size of 640×480 in pixel. The AFM cantilever in this experiment was NANOSENSORS ATEC-FM. The translation DOFs were Attocube piezoelectric ECSx3030 (1 nm resolution), representing x_M, y_M and z_M-axis. The rotation DOF mounted on y_M-axis was Attocube piezoelectric ECR3030 (1×10^{-6} degree resolution).

This article has been accepted for publication in IEEE Control Systems Letters. This is the author's version which has not been fully edited and content may change prior to final publication. Citation information: DOI 10.1109/LCSYS.2023.3336545

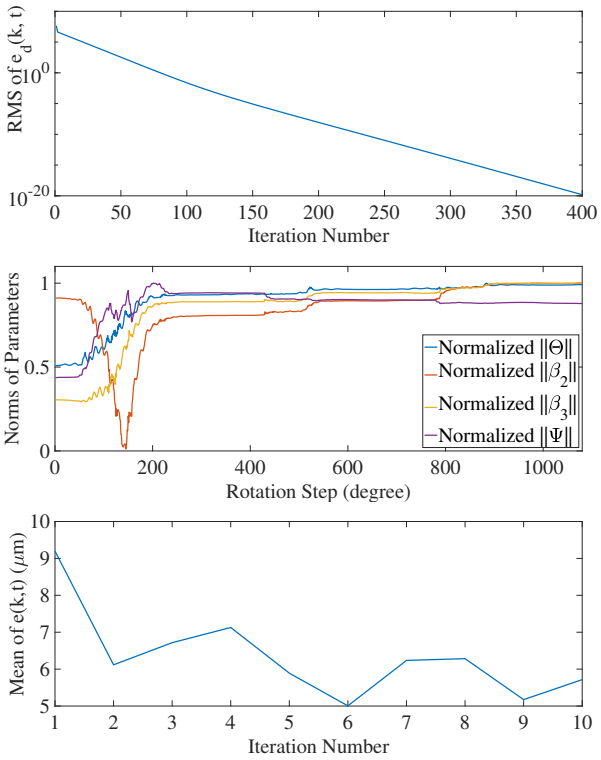

Fig. 4. Convergence Performance of IL-CMARC Scheme. (Top) Iterative convergence of $\boldsymbol{e_d(k,t)}$. (Middle) Convergence of $\boldsymbol{\Theta}$, $\boldsymbol{\beta_1}$, $\boldsymbol{\beta_2}$ and $\boldsymbol{\Psi}$. (Bottom) Iterative convergence of mean of $\boldsymbol{e(k,t)}$ per round.

The off-axis rotating experiments were implemented with a control step of 1 degree, and each iteration of rotation consisted of 360 control steps. The affixed cantilever was observed under SEM at a magnification of 500. The image Jacobian matrix of the robot system was calibrated as follows.

$$J = \begin{bmatrix} 0.0001 & 0.0026 & -0.0001 \\ 0.0026 & -0.0001 & -0.0000 \end{bmatrix}$$

B. In-situ Rotating Experiment

The nominal model of the nanorobot is identified as

$$A_0 = \begin{bmatrix} 0.9998 & -0.0002 & -0.0175 \\ 0.0002 & 1.0000 & -0.0002 \\ 0.0175 & 0.0002 & 0.9998 \end{bmatrix}, B_0 = \begin{bmatrix} 1 & 0 & 0 \\ 0 & 1 & 0 \\ 0 & 0 & 1 \end{bmatrix}$$

$$C_0 = \begin{bmatrix} 0.0001 & 0.0026 & -0.0001 \\ 0.0026 & -0.0001 & -0.0000 \end{bmatrix}, \ x_0 = \begin{bmatrix} 396123 \\ 0 \\ 214680 \end{bmatrix} nm$$

Parameters of the proposed scheme were chosen as: $A_r = \text{diag}\{-0.3, -0.5, -0.7\}$, $K_r = \text{diag}\{0.1, 0.1, 0.1\}$, $D = \text{diag}\{0.2, 0.2, 0.2\}$, $\Gamma = \text{diag}\{500, 500, 500\}$, $\Gamma_{\beta_2} = 1.2$, $\Gamma_{\beta_3} = \text{diag}\{1.1, 1.1\}$, $h(z) = 0.6321/(z - 0.3679)$. Appropriate initial values were assigned to $\beta_i(t)$, $\Theta(t)$, and $\Psi(t)$. The signal regressor was specified as $\phi(x,t) = [x(t), \sin(t), 1]^\top$. The reference signal $r(t)$ was obtained by 400 iterations offline IL-Loop running on the nominal model.

As observed in Fig. 4, the offline IL-Loop greatly enhances the online CMARC-loop convergence performance, as the offline IL requires around 150 iterations to reach $10\mu m$ precision, while the online adaption error achieved $9\mu m$ precision from the beginning. Further, due to the time delay and duration of capturing SEM images, each control step of 1 degree requires nearly 1 second to capture a high-quality SEM image and 0.1 milliseconds to implement control process, leading to one iteration costing roughly 6 minutes. This makes the pure online ILC infeasible and validates the necessity of the proposed offline IL-loop. Simulation results also conform to the same conclusion (see SM Section VI).

Fig. 5 illustrates the control performance of IL-CMARC during one round in-situ rotation. As can be seen, the average misalignment error was about 5 microns, while the standard deviation of the misalignment errors was about 4 microns. Fig. 5 bottom shows the tip trajectory on the image plane, while Fig. 6 shows the sequential images during one round rotation by every 30 degrees.

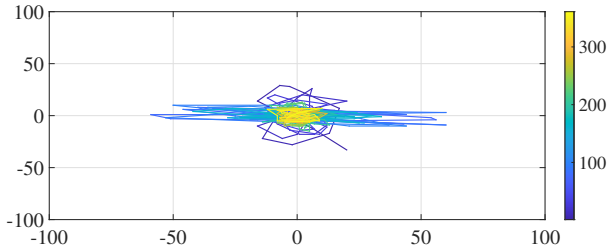

Fig. 5. In-situ rotating experiment results.

TABLE I
COMPARATIVE RESULT OF OFF-AXIS ROTATION

Control method	nRound	Avg. error (μm)	Max. error (μm)	Std. error (μm)
IL-CMARC	1	9.1968	60.3059	9.5250
	3	6.7168	48.2676	6.4325
	6	**5.0055**	**29.0269**	**4.1723**
PID	/	9.7652	29.6000	4.7173
MPC	/	7.2595	36.4198	5.5956

C. Comparative Experiments

Next, we compare the proposed method with proportional-integral-derivative (PID) control ($K_P = 0.5$ and $K_D = 0.1$) and model predictive control (MPC) (the weight matrices are set to be $\text{diag}\{2, 2, 2\}$ and $\text{diag}\{10, 10, 10\}$) to further illustrate the superior performance of the proposed method.

Statistical results of the comparative experiments were provided in Table I. It can be seen that: the proposed IL-CMARC method outperformed the other two control methods in terms of average error, maximum error and standard deviation. The results of tracking error $e(t)$ on the image plane in different control methods are illustrated in Fig. 7.

Also, it is worth mentioning that, as the results shown in Section VI in Supplement Material, purely CMARC and purely ILC are incapable of solving the rotation task. Conventional CMARC can only guarantee that $y(k,t)$ converges to $y_r(k,t)$ rather than converges to $y_d(t)$ directly. Correspondingly, by incorporating the concept of the reference model in CMARC, the stringent repeatability requirements in traditional ILC have been removed.

V. CONCLUSIONS

In this letter, we proposed an IL-CMARC scheme for the efficient visual servo to solve the problem of in-situ off-axis

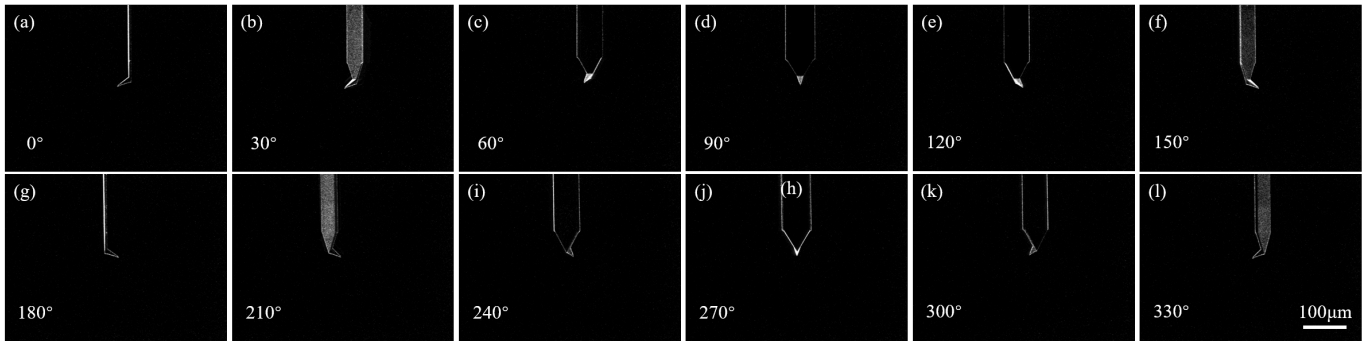

Fig. 6. SEM images of the rotating experiment of cantilever tip about rotation axis with rotation range of 360° and rotation step size of 1°. The magnification is 1000 and the length of the scale bar is 100 μm. The AFM cantilver used here is NANOSENSORS ATEC-FM.

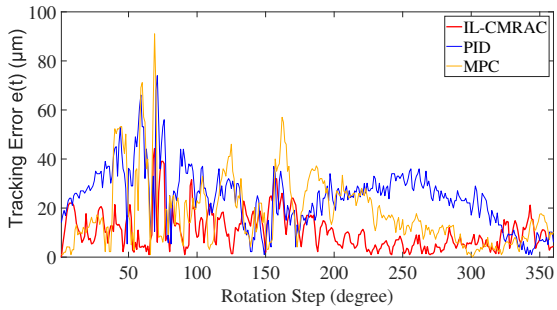

Fig. 7. Result of Different control methods for off-axis rotation.

rotation. By decoupling the ILC-loop and CMARC-loop in the iterative and time directions, the proposed method can first run in a "virtual" model to circumvent the strict repetitive limitations. Then, by reusing the stabilized nominal model and the trained signal, the presented framework preserves its advantages (direct tracking and good adaptation ability). The effectiveness of the proposed scheme is verified by extensive simulation (see SM) and a nanorobotic system with SEM.

REFERENCES

[1] Q. Yang, L. Ma, S. Xiao, D. Zhang, A. Djoulde, M. Ye, Y. Lin, S. Geng, X. Li, T. Chen, and L. Sun, "Electrical conductivity of multiwall carbon nanotube bundles contacting with metal electrodes by nano manipulators inside sem," *Nanomaterials*, vol. 11, no. 5, 2021.

[2] S. Zhuang, C. Dai, G. Shan, C. Ru, Z. Zhang, and Y. Sun, "Robotic rotational positioning of end-effectors for micromanipulation," *IEEE Transactions on Robotics*, vol. 38, no. 4, pp. 2251–2261, 2022.

[3] W. Shang, H. Lu, Y. Yang, and Y. Shen, "7-dofs rotation-thrust micro-robotic control for low-invasive cell pierce via impedance compensation," *IEEE/ASME Transactions on Mechatronics*, vol. 27, no. 6, pp. 5095–5106, 2022.

[4] H. Lu, F. Xue, W. Wan, and Y. Shen, "Investigation of scaling effect of copper microwire based on in-situ nanorobotic twisting inside sem," in *2018 IEEE International Conference on Robotics and Automation (ICRA)*, 2018, pp. 3461–3466.

[5] H. Lu, W. Shang, H. Xie, and Y. Shen, "Ultrahigh-precision rotational positioning under a microscope: Nanorobotic system, modeling, control, and applications," *IEEE Transactions on Robotics*, vol. 34, no. 2, pp. 497–507, 2018.

[6] J. Qiao, H. Wu, and X. Yu, "High-precision attitude tracking control of space manipulator system under multiple disturbances," *IEEE Transactions on Systems, Man, and Cybernetics: Systems*, vol. 51, no. 7, pp. 4274–4284, 2021.

[7] P. Pakshin, J. Emelianova, E. Rogers, and K. Galkowski, "Iterative learning control of stochastic linear systems with reference trajectory switching," in *2021 60th IEEE Conference on Decision and Control (CDC)*, 2021, pp. 6572–6577.

[8] D. Meng and K. L. Moore, "Robust iterative learning control for non-repetitive uncertain systems," *IEEE Transactions on Automatic Control*, vol. 62, no. 2, pp. 907–913, 2017.

[9] E. Lavretsky, "Combined/composite model reference adaptive control," *IEEE Transactions on Automatic Control*, vol. 54, no. 11, pp. 2692–2697, 2009.

[10] K. Guo and Y. Pan, "Composite adaptation and learning for robot control: A survey," *Annual Reviews in Control*, vol. 55, pp. 279–290, 2023.

[11] Y. Pan and H. Yu, "Composite learning robot control with guaranteed parameter convergence," *Automatica*, vol. 89, pp. 398–406, 2018.

[12] M. Yu and S. Chai, "Adaptive iterative learning control for discrete-time nonlinear systems with multiple iteration-varying high-order internal models," *International Journal of Robust and Nonlinear Control*, vol. 31, no. 15, pp. 7390–7408, 2021.

[13] J. Zhang and D. Meng, "Iterative rectifying methods for nonrepetitive continuous-time learning control systems," *IEEE Transactions on Cybernetics*, vol. 53, no. 1, pp. 338–351, 2023.

[14] Y.-C. Wang, C.-J. Chien, and I.-H. Jhuo, "Model reference adaptive iterative learning control for nonlinear systems using observer design," in *2014 IEEE International Conference on Fuzzy Systems (FUZZ-IEEE)*, 2014, pp. 1713–1719.

[15] S. Jingzhuo and W. Huang, "Model reference adaptive iterative learning speed control for ultrasonic motor," *IEEE Access*, vol. 8, pp. 181 815–181 824, 2020.

[16] Y. Yang, T. Li, X. Fu, Z. Sun, Y. F. Li, and S. Liu, "Zooming-free hand-eye self-calibration for nanorobotic manipulation inside sem," *IEEE Transactions on Nanotechnology*, vol. 22, pp. 291–300, 2023.

[17] J. Guo and G. Tao, "A discrete-time multivariable mrac scheme applied to a nonlinear aircraft model with structural damage," *Automatica*, vol. 53, pp. 43–52, 2015.

[18] D. WANG, "Convergence and robustness of discrete time nonlinear systems with iterative learning control," *Automatica*, vol. 34, no. 11, pp. 1445–1448, 1998.

[19] J. Guo, G. Tao, and Y. Liu, "A multivariable mrac scheme with application to a nonlinear aircraft model," *Automatica*, vol. 47, no. 4, pp. 804–812, 2011.

[20] J. M. Kanieski, R. V. Tambara, H. Pinheiro, R. Cardoso, and H. A. Gründling, "Robust adaptive controller combined with a linear quadratic regulator based on kalman filtering," *IEEE Transactions on Automatic Control*, vol. 61, no. 5, pp. 1373–1378, 2016.

[21] Z.-L. Zhao and B.-Z. Guo, "A nonlinear extended state observer based on fractional power functions," *Automatica*, vol. 81, pp. 286–296, 2017.

[22] G. Tao, *Adaptive control design and analysis*. New York: John Wiley and Sons, 2003.

[23] J. Liu, X. Ruan, and Y. Zheng, "Iterative learning control for discrete-time systems with full learnability," *IEEE Transactions on Neural Networks and Learning Systems*, vol. 33, no. 2, pp. 629–643, 2022.